

Spontaneous emission mediated by cooperative energy transfer to plasmonic antenna

Tigran V. Shahbazyan

Department of Physics, Jackson State University, Jackson, MS 39217 USA

Spontaneous emission from ensembles of quantum emitters (QEs) such as atoms, molecules, or semiconductor quantum dots can be greatly accelerated due to cooperative behavior arising from electromagnetic correlations between them. We describe new cooperative emission mechanism mediated by cooperative energy transfer (CET) from QEs to localized surface plasmon in metal-dielectric structure. The transferred energy is radiated away by the plasmonic antenna at rate that equals the sum of individual QE emission rates. For large QE ensembles saturating the plasmon mode volume, we derive universal, i.e., independent of local field distribution, expression for cooperative Purcell factor that far exceeds the field enhancement limits for individual QE in a hot spot. We also derive radiated power spectrum that retains the plasmon resonance lineshape and, in contrast to common cooperative mechanisms, is insensitive to natural variations of QEs' emission frequencies.

Surface plasmons are collective electronic excitations that can be resonantly excited in metal-dielectric structures with characteristic size well below the diffraction limit [1]. Rapid oscillations of electron charge density at metal-dielectric interfaces generate extremely strong alternating local fields that can dramatically affect optical properties of nearby dye molecules or semiconductor quantum dots, hereafter referred to as quantum emitters (QEs) [2–5]. Optical interactions between QEs and plasmons give rise to a number of major phenomena such as surface-enhanced Raman scattering (SERS) [6], plasmon-enhanced fluorescence and luminescence [7–9], plasmon-assisted energy transfer [10–13], strong QE-plasmon coupling [14–20] and plasmonic laser (spaser) [21–23].

Plasmonic enhancement of spontaneous emission from a QE near a plasmonic structure is a generic effect that underpins much of plasmon-enhanced spectroscopy phenomena and many plasmonics applications [24–30]. The enhancement is rooted in highly efficient energy transfer (ET) from QE, located in the strong local field region, to localized plasmon in metal-dielectric structure followed by plasmon radiative decay (antenna effect) [31–37]. The local field enhancement of decay rate, usually described by the Purcell factor [38], can reach several orders of magnitude, e.g., near sharp metal tips, but is still limited by Ohmic losses and nonlocal effects in metals [40, 41].

On the other hand, light emission from an *ensemble* of QEs can be greatly accelerated due to cooperativity arising from correlations between QEs. A prominent example is Dicke superradiance of QEs, interacting with common radiation field, which occurs at rate scaling with the ensemble size [42, 43]. If QEs are placed near plasmonic structure, the radiation coupling is enhanced due to strong local fields [44–51] thereby reducing the adverse effect of dipole-dipole coupling [52, 53]. At the same time, the Ohmic losses suppress correlations near the metal surface, where the local fields are strongest [44, 45]. Notwithstanding recent reports [54, 55], observation of plasmon-enhanced superradiance remains a challenge as it hinges on delicate interplay between direct dipole coupling, plasmonic correlations, and metal losses.

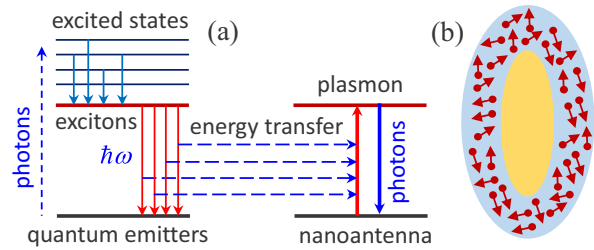


FIG. 1. (a) Schematics of CET from QE ensemble to plasmonic antenna. (b) Schematics of plasmonic system with QEs distributed within dielectric shell surrounding metallic core.

In this paper, we describe new mechanism of cooperative emission based on *cooperative energy transfer* (CET) from ensemble of QEs to plasmonic antenna (see Fig. 1). We demonstrate that excited QEs resonantly coupled to a single plasmon mode form collective state that transfers its energy cooperatively to plasmon at rate equal to the sum of individual QE-plasmon ET rates. The transferred energy is radiated away by plasmonic antenna at rate that scales with the number of QEs involved in CET. We derive the cooperative Purcell factor describing plasmonic enhancement of the ensemble decay rate and show that, for QEs saturating the plasmon mode volume, it has universal form independent of local field distribution in metal-dielectric structure. We also derive an explicit expression for radiated power spectrum that retains the plasmon resonance lineshape with overall amplitude proportional to the cooperative Purcell factor. Importantly, the CET mechanism is insensitive to natural QE frequency variations due to, e.g., direct dipole-dipole coupling, if they stay within broad plasmon absorption band, in contrast with common cooperative mechanisms, such as superradiance, where even weak disorder in QE frequencies strongly alters the emission spectra [52, 53]. Below we outline our theory for CET-mediated cooperative emission and present numerical results indicating that cooperative rate enhancement exceeds by far the local field enhancement limits for individual QEs in hot spot.

Theory.—We start with spontaneous decay of *single* QE coupled to a plasmonic resonator represented by

metal-dielectric nanostructure characterized by complex dielectric function $\varepsilon(\omega, \mathbf{r}) = \varepsilon'(\omega, \mathbf{r}) + i\varepsilon''(\omega, \mathbf{r})$. We assume that characteristic system size is much smaller than the radiation wavelength so that the plasmon electric field $\mathbf{E}(\mathbf{r})$, which we chose to be real, and frequency ω_{pl} satisfy the quasistatic Gauss law $\nabla \cdot [\varepsilon'(\omega_{pl}, \mathbf{r}) \mathbf{E}(\mathbf{r})] = 0$ with standard boundary conditions [5]. The decay rate of QE located at \mathbf{r}_0 is given by $\gamma = (2/\hbar) \text{Im}[\mathbf{p}^* \cdot \mathbf{E}(\mathbf{r}_0)]$, where $\mathbf{E}(\mathbf{r}) = \bar{\mathbf{D}}(\omega; \mathbf{r}, \mathbf{r}_0) \cdot \mathbf{p}$ is the electric field of QE's oscillating dipole $\mathbf{p}e^{-i\omega t} = \mu \mathbf{n} e^{-i\omega t}$, where μ and \mathbf{n} are dipole moment and orientation, respectively, and $\bar{\mathbf{D}}(\omega; \mathbf{r}, \mathbf{r}') = (4\pi\omega^2/c^2) \bar{\mathbf{G}}(\omega; \mathbf{r}, \mathbf{r}')$ is the electromagnetic Green function ($\bar{\mathbf{G}}$ is the standard dyadic Green function for Maxwell equation including plasmonic system [56]).

In the *near field* limit, the Green function can be split into free-space and plasmon parts, $\bar{\mathbf{D}} = \bar{\mathbf{D}}_0 + \bar{\mathbf{D}}_{pl}$, and accordingly, the QE decay rate has the form $\gamma = \gamma_0^r + \gamma_{et}$, where $\gamma_0^r = 4\mu^2\omega^3/3\hbar c^3$ is free-space decay rate [56] and

$$\gamma_{et} = \frac{2\mu^2}{\hbar} \text{Im} [\mathbf{n} \cdot \bar{\mathbf{D}}_{pl}(\omega; \mathbf{r}_0, \mathbf{r}_0) \cdot \mathbf{n}] \quad (1)$$

is the ET rate from QE to plasmon. Part of transferred energy is radiated away by the plasmonic antenna at rate that is determined by plasmon's radiation efficiency while the rest is dissipated in the metal. These processes are included in the plasmon Green function, which, for ω close to plasmon frequency ω_{pl} , has the form [37, 39]

$$\bar{\mathbf{D}}_{pl}(\omega; \mathbf{r}, \mathbf{r}') = \frac{\omega_{pl}}{4U_{pl}} \frac{\mathbf{E}(\mathbf{r}) \mathbf{E}(\mathbf{r}')}{\omega_{pl} - \omega - i\gamma_{pl}/2}, \quad (2)$$

where $\gamma_{pl} = W_{pl}/U_{pl}$ is the plasmon decay rate. Here,

$$U_{pl} = \frac{1}{16\pi} \int dV \frac{\partial[\omega_{pl} \varepsilon'(\omega_{pl}, \mathbf{r})]}{\partial \omega_{pl}} \mathbf{E}^2(\mathbf{r}) \quad (3)$$

is plasmon mode energy and $W_{pl} = W_{pl}^{nr} + W_{pl}^r$ is power dissipated by the plasmon due to nonradiative (W_{pl}^{nr}) and radiative (W_{pl}^r) losses. The Ohmic contribution has the form $W_{pl}^{nr} = (\omega_{pl}/8\pi) \int dV \varepsilon''(\omega_{pl}, \mathbf{r}) \mathbf{E}^2(\mathbf{r})$ [57]. Since integration in W_{pl}^{nr} and U_{pl} is, in fact, restricted to metal regions with dielectric function $\varepsilon(\omega) = \varepsilon'(\omega) + i\varepsilon''(\omega)$, the standard plasmon nonradiative decay rate follows, $\gamma_{pl}^{nr} = W_{pl}^{nr}/U_{pl} = 2\varepsilon''(\omega_{pl})/[\partial\varepsilon'(\omega_{pl})/\partial\omega_{pl}]$. At the same time, if plasmonic system is smaller than the radiation wavelength, power *radiated* by the plasmon is similar to that of localized dipole, $W_{pl}^r = (\omega_{pl}^4/3c^3)\mathcal{P}^2$, where $\mathcal{P} = \int dV \mathbf{E}(\mathbf{r}) \chi(\omega_{pl}, \mathbf{r})$ is plasmon's dipole moment and $\chi(\omega_{pl}, \mathbf{r}) = [\varepsilon'(\omega_{pl}, \mathbf{r}) - 1]/4\pi$ is plasmonic system's susceptibility [37]. Accordingly, the plasmon radiative decay rate $\gamma_{pl}^r = W_{pl}^r/U_{pl}$ defines the radiation efficiency of single-mode plasmonic antenna: $\eta = \gamma_{pl}^r/(\gamma_{pl}^{nr} + \gamma_{pl}^r)$.

The QE-plasmon ET rate is obtained by substituting the plasmon Green function (2) into Eq. (1),

$$\gamma_{et}^c(\omega) = \frac{\mu^2 Q}{\hbar U_{pl}} \frac{[\mathbf{n} \cdot \mathbf{E}(\mathbf{r}_0)]^2}{1 + 4Q^2(\omega/\omega_{pl} - 1)^2}, \quad (4)$$

where $Q = \omega_{pl}/\gamma_{pl}$ is plasmon quality factor. The maximal enhancement of QE's decay rate at resonance $\omega = \omega_{pl}$ is traditionally presented as $\gamma(\omega_{pl}) = \gamma_0^r(1 + F)$, where F is the Purcell factor. Introducing plasmon mode volume at point \mathbf{r} projected along \mathbf{n} as [37]

$$\frac{1}{\mathcal{V}_n(\mathbf{r})} = \frac{2[\mathbf{n} \cdot \mathbf{E}(\mathbf{r})]^2}{\int dV \mathbf{E}^2 \partial(\omega_{pl} \varepsilon')/\partial \omega_{pl}}, \quad (5)$$

the Purcell factor for plasmonic resonators takes the form

$$F = \frac{6\pi Q}{k^3 \mathcal{V}_n} = \frac{12\pi Q [\mathbf{n} \cdot \mathbf{E}(\mathbf{r}_0)]^2}{k^3 \int dV \mathbf{E}^2 \partial(\omega_{pl} \varepsilon')/\partial \omega_{pl}}, \quad (6)$$

where we denoted $\varepsilon \equiv \varepsilon(\omega_{pl}, \mathbf{r})$ in the integrand. The enhancement factor for radiated power spectrum is $M(\omega) = [\gamma_{et}(\omega)/\gamma_0^r]\eta$, with maximal enhancement $M(\omega_{pl}) = F\eta$.

Let us now turn to light emission from *ensemble* of N excited QEs at positions \mathbf{r}_i near plasmonic structure. We assume incoherent excitation, i.e., QEs' dipole moments $\mathbf{p}_i = \mu \mathbf{n}_i e^{i\phi_i}$ contain random phases ϕ_i simulating uncorrelated initial states. Each excited QE couples to the *common* electric field as $\mathbf{p}_i^* \cdot \mathbf{E}(\mathbf{r}_i)$, where the field

$$\mathbf{E}(\mathbf{r}) = \sum_j \bar{\mathbf{D}}(\omega; \mathbf{r}, \mathbf{r}_j) \cdot \mathbf{p}_j, \quad (7)$$

is generated by *all* QEs, implying that the system eigenstates are determined by the Green function matrix between QEs' positions [43]: $D_{ij} = \hbar^{-1} \mathbf{p}_i^* \cdot \bar{\mathbf{D}}(\omega; \mathbf{r}_i, \mathbf{r}_j) \cdot \mathbf{p}_j$.

Following near-field decomposition of the dyadic Green function $\bar{\mathbf{D}}$, the coupling matrix \hat{D} can be split into free-space and plasmon parts, $D_{ij} = D_{ij}^0 + D_{ij}^{pl}$, where D_{ij}^{pl} describes plasmon-assisted correlations between QEs and, near the resonance, dominates over free-space coupling D_{ij}^0 , which mainly accounts for dipole-dipole interactions between QEs and will be neglected for now. With plasmon Green function (2), the coupling takes the form

$$D_{ij}^{pl}(\omega) = \frac{\omega_{pl}}{4\hbar U_{pl}} \frac{\mathbf{p}_i^* \cdot \mathbf{E}(\mathbf{r}_i) \mathbf{p}_j \cdot \mathbf{E}(\mathbf{r}_j)}{\omega_{pl} - \omega - i\gamma_{pl}/2}, \quad (8)$$

where diagonal elements $D_{ii} = \delta\omega^{(i)} + i\gamma_{et}^{(i)}/2$ include frequency shifts $\delta\omega^{(i)}$ and QE-plasmon ET rates $\gamma_{et}^{(i)}$ for individual QEs [see Eq. (4)]. Eigenstates of the matrix (8) describe collective states formed due to plasmonic correlations between QEs, while the corresponding eigenvalues describe those states' frequency shifts and decay rates.

It is easy to see that collective state presented by the vector $\psi_c = \{\mathbf{p}_1^* \mathbf{E}_m(\mathbf{r}_1), \dots, \mathbf{p}_N^* \mathbf{E}_m(\mathbf{r}_N)\}$ is eigenstate of the matrix (8) that *saturates* ET from QEs to plasmon. Indeed, its eigenvalue has the form $\delta\omega^c + i\gamma_{et}^c/2$, where

$$\gamma_{et}^c = \sum_i \gamma_{et}^{(i)}, \quad \delta\omega^c = \sum_i \delta\omega^{(i)}, \quad (9)$$

are, respectively, the collective state's decay rate and frequency shift. The rest of eigenstates are uncoupled from the plasmon but, in principle, can radiate on their own.

We have thus established that, due to plasmonic correlations, a collective state of N excited QEs transfers its energy *cooperatively* at rate that equals the sum of individual QE-plasmon ET rates. Using Eq. (4) for individual rates, the CET rate takes the form

$$\gamma_{et}^c(\omega) = \frac{\mu^2 Q}{\hbar U_{pl}} \sum_i \frac{[\mathbf{n}_i \cdot \mathbf{E}(\mathbf{r}_i)]^2}{1 + 4Q^2(\omega/\omega_{pl} - 1)^2}. \quad (10)$$

Normalizing the CET rate at resonance $\gamma_{et}^c(\omega_{pl})$ by γ_r^r , we obtain cooperative Purcell factor

$$F_c = \sum_i \frac{6\pi Q}{k^3 \mathcal{V}_n^{(i)}} = \sum_i \frac{12\pi Q_m |\mathbf{n}_i \cdot \mathbf{E}_m(\mathbf{r}_i)|^2}{k^3 \int dV |\mathbf{E}_m|^2 \partial(\omega_m \varepsilon')/\partial \omega_m} \quad (11)$$

as the sum of Purcell factors (6) for individual QEs.

Let us turn to power spectrum radiated by N excited QEs via CET to plasmonic antenna. The full radiated power W_r is obtained by integrating Poynting's vector $\mathbf{S} = (c/8\pi)|\mathbf{E}(\mathbf{r})|^2$ over remote surface enclosing the system, where $\mathbf{E}(\mathbf{r})$ is the far field generated by QEs. To extract the far field contribution from Eq. (7), we use the Dyson equation for Green function, $\bar{\mathbf{D}} = \bar{\mathbf{D}}_0 + \bar{\mathbf{D}}_0 \cdot \chi \bar{\mathbf{D}}$. Near the resonance, by replacing $\bar{\mathbf{D}}$ with the plasmon Green function (2), we obtain after some algebra

$$W_r = \frac{\omega^4}{3c^3} \left| \sum_i \left[\mathbf{p}_i + \frac{\omega_{pl}}{4U_{pl}} \frac{\mathbf{P}[\mathbf{E}(\mathbf{r}_i) \cdot \mathbf{p}_i]}{\omega_{pl} - \omega - i\gamma_{pl}/2} \right] \right|^2, \quad (12)$$

where the second term describes contribution of the antenna with dipole moment \mathbf{P} . After averaging out over random phases in $\mathbf{p}_i = \mu \mathbf{n}_i e^{i\phi_i}$ and neglecting nonresonant direct QE emission (first term), we obtain radiated power spectrum mediated by CET to plasmonic antenna

$$W_r^c = \frac{\mu^2 \omega^4}{3c^3} \frac{\gamma_{pl}^r \gamma_{et}^c(\omega)}{\gamma_{pl} \gamma_r^r}, \quad (13)$$

where CET rate $\gamma_{et}^c(\omega)$ is given by Eq. (10). Finally, the cooperative enhancement factor for radiated power spectrum is obtained by normalizing W_r^c with individual QE's radiated power $W_r^0 = \mu^2 \omega^4 / 3c^3$ [56],

$$M_c(\omega) = \frac{W_r^c}{W_r^0} = \frac{F_c \eta}{1 + 4Q^2(\omega/\omega_{pl} - 1)^2}. \quad (14)$$

At resonance, the enhancement factor is $M_c(\omega_{pl}) = F_c \eta$.

Discussion.—A distinct feature of CET-based cooperative emission is its robust power spectrum that retains plasmon resonance lineshape with overall amplitude scaling with the ensemble size. This spectral stability contrasts common cooperative mechanisms, e.g., superradiance, where light emanates directly from the QEs, rather than the antenna, and hence any changes in the decay rate affect the emission linewidth. Furthermore, CET to plasmon is largely insensitive to QE frequency variations due to, e.g., direct dipole-dipole coupling, if they

fit within broad plasmon band, in contrast to, e.g., superradiance, where even weak disorder drastically affects the emission spectra [52, 53]. Note that for large QE ensembles, quenching effects that hinder single-QE emission near the metal surface are largely suppressed [59, 60].

We stress that CET-based cooperative emission is *weak* coupling effect that does not require plasmon reabsorption, unlike strong coupling regime characterized by coherent QE-plasmon energy exchange [14–20]. Excited QEs that are coupled to a *single* plasmon mode undergo CET if their *emission* spectrum overlaps with plasmon absorption band. If QE's absorption band is well above its emission peak, the energy transferred to plasmonic antenna is radiated away at rate that scales with the number of *excited* QEs involved in CET, which can be varied in wide range with excitation power.

Let us analyze CET scenarios for common QEs distributions near plasmonic structure. If QEs are placed in a *plasmonic cavity*, e.g., within dielectric core surrounded by metallic shell, the plasmon field is nearly uniform in the QE region, and so the mode volume $\mathcal{V}_n^{(i)}$ in Eq. (16), which characterizes plasmon field localization at \mathbf{r}_i , is constant on average. In this case, the cooperative Purcell factor is simply $F_c = NF$, i.e., the ensemble spontaneous decay rate scales *linearly* with the excited QE number.

In another setup, QEs are placed *outside* the metal structure, e.g., within dielectric shell around metal core (see Fig. 1). In this case, plasmon fields decrease rapidly away from the metal surface. We assume uniform QE distribution, with random dipole orientations, in a region of volume V_0 and dielectric constant ε_d . Introducing the average mode volume in the QE region as [61]

$$\frac{1}{V_0} = \frac{1}{V_0} \frac{2 \int dV_0 \mathbf{E}^2}{\int dV \mathbf{E}^2 \partial(\omega_{pl} \varepsilon')/\partial \omega_{pl}}, \quad (15)$$

the cooperative Purcell factor takes the form

$$F_c = \frac{2\pi N Q}{k^3 V_0} = \frac{4\pi n}{k^3} \frac{Q \int dV_0 \mathbf{E}^2}{\int dV \mathbf{E}^2 \partial(\omega_{pl} \varepsilon')/\partial \omega_{pl}}, \quad (16)$$

where $n = N/V_0$ is QE concentration, and the extra factor 1/3, compared to individual Purcell factor (6), comes from orientational averaging. Note that CET-based cooperativity is characterized by parameter N/V_0 , i.e., QEs' number within average mode volume, rather than by common superradiance parameter N/V_0 [42, 43].

Since remote QEs couple weakly to the plasmon, a sufficiently large QE region *saturates* the mode volume, i.e., no significant field spillover takes place beyond this region. In this case, the integrated field intensity $\int dV_0 \mathbf{E}^2$ is independent of V_0 and so the saturated mode volume \mathcal{V}_{sat} scales with V_0 . Using the Gauss law and omitting the remote QEs' contribution [58], we obtain universal *field-independent* saturated plasmon mode volume,

$$\frac{\mathcal{V}_{\text{sat}}}{V_0} = \frac{\varepsilon_d \omega_{pl}}{2|\varepsilon'(\omega_{pl})|} \frac{\partial \varepsilon'(\omega_{pl})}{\partial \omega_{pl}}, \quad (17)$$

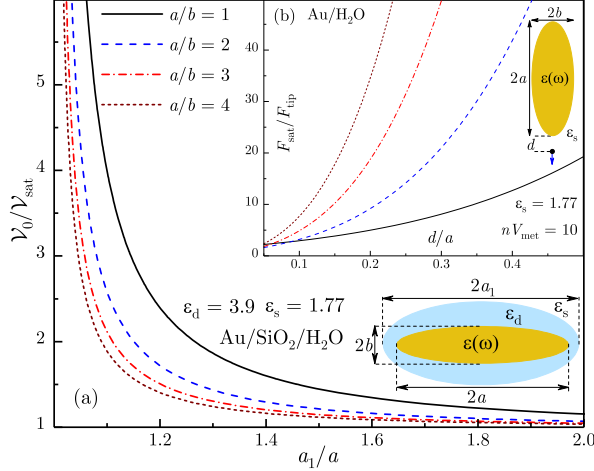


FIG. 2. (a) Average mode volume in units of saturated one is plotted vs. QE region size. (b) Cooperative enhancement vs. local field enhancement for QE at distance d from metal tip.

which depends on system geometry only via plasmon frequency ω_{pl} in the metal dielectric function. Finally, for saturated case, the cooperative Purcell factor (16) is

$$F_{\text{sat}} = \frac{2\pi NQ}{k^3 \mathcal{V}_{\text{sat}}} = \frac{4\pi nQ}{k^3 \epsilon_d} \frac{|\epsilon'(\omega_{pl})|}{\omega_{pl} \partial \epsilon'(\omega_{pl}) / \partial \omega_{pl}}. \quad (18)$$

Remarkably, cooperative Purcell factor for QE distribution saturating the plasmon mode volume is determined *solely* by experimentally measured system parameters.

As an example, we consider Au nanorods in water coated by QE-doped SiO_2 shell modeled by two confocal prolate spheroids [see schematics in Fig. 2(a)]. The inner and outer surfaces correspond to semi-major axes a and a_1 , respectively, and QE concentration $n = N/V_0$ is constant within the shell volume V_0 [58]. With extending QE region, i.e., increasing a_1/a , the average mode volume for longitudinal plasmon rapidly saturates, i.e., $\mathcal{V}_0/\mathcal{V}_{\text{sat}} \approx 1$ for relatively thin shells [see Fig. 2(a)].

In Fig. 2(b) we compare cooperative Purcell factor (18) to Purcel factor F_{tip} of a single QE placed near Au nanorod tip, where local fields are strongest [see schematics Fig. 2(b)]. Since plasmon mode volume near the tip scales with the metal volume V_{met} [37], the ratio $F_{\text{sat}}/F_{\text{tip}}$ scales with nV_{met} , but is very sensitive to QE's distance d to the tip [58]. For relatively low value $nV_{\text{met}} = 10$, i.e., number of QEs that would fit within metal volume at given QE concentration n in the shell, the cooperative enhancement of decay rate far exceeds the local field enhancement. Note that for $d < 1$ nm, the local fields are damped by nonlocal effects [40, 41].

In Fig. 3, we plot cooperative Purcell factor F_c and power spectrum enhancement factor $M_c = F_c \eta$ vs. QE region size, with increasing nanorod length at fixed aspect ratio $a/b = 3.0$, and for QE concentration $n = 1.0$ mM. Both F_c and M_c first grow with the shell thickness but then saturate as remote QEs' coupling to plasmon diminishes. Although the plasmon mode volume is nearly

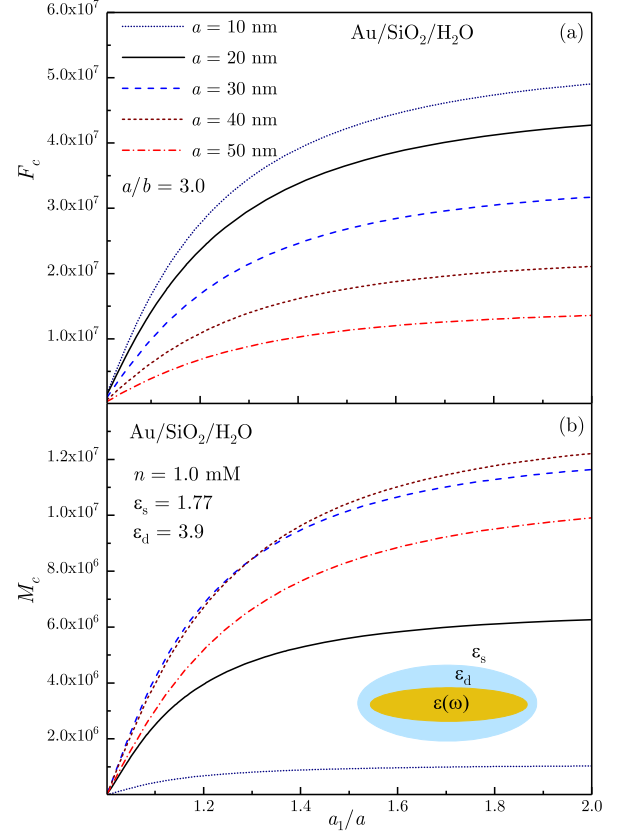


FIG. 3. Cooperative Purcell factor (a) and power spectrum enhancement factor (b) are plotted vs. QE region size with increasing nanorod length at fixed core aspect ratio $a/b = 3.0$.

saturated at $a_1/a = 2.0$ [see Fig. 2(a)], the curves still show weak size dependence due to plasmon frequency change with shell thickness. The evolution of F_c and M_c with increasing nanorod length is defined by the interplay between plasmon quality factor Q and radiation efficiency η , which change in the opposite ways with increasing γ_{pl}^r . In fact, the smallest nanorod ($a = 10$ nm) has the largest Purcell factor $F_c \propto Q$ [see Fig. 3(a)] but, at the same time, the smallest enhancement factor $M_c \propto Q\eta$, while the largest M_c are those of medium-sized rods [see Fig. 3(b)]. Note that the optimal radiation efficiency for maximal power spectrum enhancement is $\eta = 1/2$.

In summary, we described new mechanism for cooperative emission of light by an ensemble of excited QEs mediated by cooperative energy transfer to the plasmonic antenna. The cooperative emission rate scales with the number of excited QEs and, for large ensembles saturating the plasmon mode volume, has universal form independent of local field distribution in the system.

This work was supported in part by NSF grants No. DMR-1610427 and No. HRD-1547754.

[1] S. A. Maier, *Plasmonics: Fundamentals and Applications*, (Springer, New York, 2007).

[2] M. Moskovits, Rev. Mod. Phys. **57** 783 (1985) .

[3] S. A. Maier and H. A. Atwater, J. Appl. Phys. **98**, 011101 (2005).

[4] E. Ozbay, Science **311**, 189 (2006).

[5] M. I. Stockman, in *Plasmonics: Theory and Applications*, edited by T. V. Shahbazyan and M. I. Stockman (Springer, New York, 2013).

[6] E. C. Le Ru and P. G. Etchegoin, *Principles of Surface-Enhanced Raman Spectroscopy* (Elsevier, 2009).

[7] P. Anger, P. Bharadwaj, and L. Novotny, Phys. Rev. Lett. **96**, 113002 (2006).

[8] S. Kühn, U. Hakanson, L. Rogobete, and V. Sandoghdar, Phys. Rev. Lett. **97**, 017402 (2006).

[9] F. Tam, G. P. Goodrich, B. R. Johnson, and N. J. Halas, Nano Lett. **7**, 496 (2007).

[10] J. R. Lakowicz, J. Kusba, Y. Shen, J. Malicka, S. DAuria, Z. Gryczynski, I. Gryczynski, J. Fluoresc. **13**, 69 (2003).

[11] P. Andrew and W. L. Barnes, Science **306**, 1002 (2004).

[12] F. Reil, U. Hohenester, J. R. Krenn, and A. Leitner, Nano Lett. **8**, 4128 (2008).

[13] C. Blum, N. Zijlstra, A. Lagendijk, M. Wubs, A. P. Mosk, V. Subramaniam, W. L. Vos, Phys. Rev. Lett. **109**, 203601 (2012).

[14] J. Bellessa, C. Bonnand, J. C. Plenet, and J. Mugnier, Phys. Rev. Lett. **93**, 036404 (2004).

[15] Y. Sugawara, T. A. Kelf, J. J. Baumberg, M. E. Abdelsalam, and P. N. Bartlett, Phys. Rev. Lett. **97**, 266808 (2006).

[16] N. T. Fofang, T.-H. Park, O. Neumann, N. A. Mirin, P. Nordlander, and N. J. Halas, Nano Lett. **8**, 3481 (2008).

[17] D. E. Gomez, K. C. Vernon, P. Mulvaney, and T. J. Davis, Nano Lett. **10**, 274 (2010).

[18] A. Salomon, R. J. Gordon, Y. Prior, T. Seideman, and M. Sukharev, Phys. Rev. Lett. **109**, 073002 (2012).

[19] S. Aberra Guebrou, C. Symonds, E. Homeyer, J. C. Plenet, Y. N. Gartstein, V. M. Agranovich, and J. Bellessa, Phys. Rev. Lett. **108**, 066401 (2012).

[20] T. Antosiewicz, S. P. Apell, and T. Shegai, ACS Photonics, **1**, 454 (2014).

[21] D. J. Bergman and M. I. Stockman, Phys. Rev. Lett., **90**, 027402, (2003).

[22] M. I. Stockman, Nature Photon. **2**, 327, (2008).

[23] M. A. Noginov, G. Zhu, A. M. Belgrave, R. Bakker, V. M. Shalaev, E. E. Narimanov, S. Stout, E. Herz, T. Suteewong and U. Wiesner, Nature, **460**, 1110, (2009).

[24] M. Pelton, Nat. Photon. **9**, 427 (2015).

[25] G. M. Akselrod, C. Argyropoulos, T. B. Hoang, C. Ciraci, C. Fang, J. Huang, D. R. Smith, and M. H. Mikkelsen, Nat. Photon. **8**, 835 (2014).

[26] M. S. Eggleston, K. Messer, L. Zhan, E. Yablonovitch, M. C. Wu, Proc. Nat. Acad. Sci., **112**, 1704 (2015).

[27] F. D. Angelis, M. Malerba, M. Patrini, E. Miele, G. Das, A. Toma, R. P. Zaccaria, E. D. Fabrizio, Nano Lett. **13**, 3553 (2013).

[28] C.-Y. Jin, R. John, M. Y. Swinkels, T. B. Hoang, L. Midolo, P. J. van Veldhoven, A. Fiore, Nat. Nanotechnol. **9**, 886 (2014).

[29] M. Malerba, A. Alabastri, E. Miele, P. Zilio, M. Patrini, D. Bajoni, G. C. Messina, M. Dipalo, A. Toma, R. P. Zaccaria, F. D. Angelis, Sci. Rep. **5**, 16436 (2015).

[30] P. Guo, R. D. Schaller, J. B. Ketterson, and R. P. H. Chang, Nat. Photon. **10**, 267 (2016).

[31] R. Carminati, J. J. Greffet, C. Henkel, J. M. Vigoureux, Opt. Commun. **261** 368 (2006).

[32] C. Sauvan, J. P. Hugonin, I. S. Maksymov, and P. Lalanne, Phys. Rev. Lett. **110**, 237401 (2013).

[33] A. E. Krasnok, A. P. Slobozhanyuk, C. R. Simovski, S. A. Tretyakov, A. N. Poddubny, A. E. Miroshnichenko, Y. S. Kivshar, and P. A. Belov, Sci. Rep. **5**, 12956 (2015).

[34] F. Marquier, C. Sauvan, and J.-J. Greffet, ACS Phot. **4**, 20912101 (2017).

[35] A. F. Koenderink, ACS Phot. **4**, 710-722 (2017).

[36] P. Lalanne, W. Yan, K. Vynck, C. Sauvan, and J.P. Hugonin, Laser Photon. Rev. **12**, 1700113 (2018).

[37] T. V. Shahbazyan, arXiv:1805.09529.

[38] E. M. Purcell, Phys. Rev. **69** 681 (1946).

[39] T. V. Shahbazyan, Phys. Rev. Lett. **117**, 207401 (2016).

[40] C. Ciraci, R. T. Hill, J. J. Mock, Y. Urzumov, A. I. Fernández-Domnguez, S. A. Maier, J. B. Pendry, A. Chilkoti, and D. R. Smith, Science **337**, 1072 (2012).

[41] N. A. Mortensen, S. Raza, M. Wubs, T. Søndergaard, and S. I. Bozhevolnyi, Nat. Commun. **5**, 3809 (2014).

[42] R. H. Dicke, Phys. Rev. **93**, 99 (1954).

[43] M. Gross and S. Haroche, Phys. Rep. **93**, 301 (1982).

[44] V. N. Pustovit, T. V. Shahbazyan, Phys. Rev. Lett. **102**, 077401 (2009).

[45] V. N. Pustovit, T. V. Shahbazyan, Phys. Rev. B **82**, 075429 (2010).

[46] D. Martin-Cano, L. Martin-Moreno, F. J. Garcia-Vidal, and E. Moreno, Nano Lett. **10**, 3129 (2010).

[47] J. J. Choquette, K.-P. Marzlin, and B. C. Sanders, Phys. Rev. A **82**, 023827 (2010).

[48] V. N. Pustovit, A. M. Urbas, T. V. Shahbazyan, Phys. Rev. B **88**, 245427 (2013).

[49] Y. Zhang and V. May, Phys. Rev. B **89**, 245441 (2014).

[50] N. J. Schilder, C. Sauvan, J.-P. Hugonin, S. Jennewein, Y. R. P. Sortais, A. Browaeys, and J.-J. Greffet, Phys. Rev. A **93**, 063835 (2016).

[51] P. Fauché, S. G. Kosionis, and P. Lalanne, Phys. Rev. B **95**, 195418 (2017).

[52] R. Friedberg, S. R. Hartmann, and J. T. Manassah, Phys. Rep. C **7**, 101 (1973).

[53] T. V. Shahbazyan, M. E. Raikh, and Z. V. Vardeny, Phys. Rev. B **61**, 13266 (2000).

[54] L. N. Tripathi, M. Praveena, and J. K. Basu, Plasmonics, **8**, 657 (2013).

[55] M. V. Shestakov, E. Fron, L. F. Chibotaru, and V.V. Moshchalkov, J. Phys. Chem. C **119**, 20051 (2015).

[56] L. Novotny and B. Hecht, *Principles of Nano-Optics* (CUP, New York, 2012).

[57] L. D. Landau and E. M. Lifshitz, *Electrodynamics of Continuous Media* (Elsevier, Amsterdam, 2004).

[58] See Supplemental Material.

[59] A. Delga, J. Feist, J. Bravo-Abad, and F.J. Garcia-Vidal, Phys. Rev. Lett. **112**, 253601 (2014).

[60] L. S. Petrosyan and T. V. Shahbazyan, Phys. Rev. B **96**, 075423 (2017).

[61] T. V. Shahbazyan, ACS Photon. **4**, 1003 (2017).